# Magnetic Multilayer Fabrication Technology with Selective Activation of SU-8 Films



2016 J. Phys.: Conf. Ser. 757 012031

(http://iopscience.iop.org/1742-6596/757/1/012031)

# Magnetic Multilayer Fabrication Technology with Selective Activation of SU-8 Films

**R Anthony**[1, 2], **C ÓMathúna**[1, 2] **and JF Rohan**[1]
[1]Tyndall National Institute, Lee Maltings, University College, Cork, Cork, Ireland
[2]Electrical and Electronics Engineering, University College Cork, Cork, Ireland

**Abstract.** Developing magnetic multilayers are essential for reducing the core eddy current losses in the integrated power magnetic components (inductors/transformers). PVD based processes are typically used to achieve the multilayers with thin dielectric spacers. However, those processes are costly, and can be difficult to integrate. It is evident that cost effective alternative is needed. In recent years, electrochemical processes have been investigated to address these issues. One such method would be to successive metallization of insulating photoresists acting as spacer layer (such as SU-8) with soft magnetic films (such as Ni-Fe-Co alloys). This paper describes an experimental procedure to fabricate magnetic multilayers with a thin variant of SU-8 2 (< 1.5 µm) as inter-layers for integrated micro-inductors/transformers for power conversion applications.

## 1. Introduction

The power conversion circuitry is an integral part of any portable electronics. A major section of the circuitry is the energy storage and transfer passive components (inductors and transformers) which are often bulky and non-integratable. Increasing in the switching frequency of the DC-DC power converters in recent years has reduced inductance (and energy storage) requirements, thus these passives can now be fabricated on silicon with MEMS-based processes [1]. However, with the continuous reduction and increase in functionality of portable electronics, it is apparent that these components be further miniaturized without compromising on efficiency. To meet required device specification in a limited footprint is challenging. Although increase in switching frequencies have reduced footprint, increasing magnetic core flux density could also increase inductance density. This would potentially reduce the number of windings in the device and thus reduce the overall footprint area. Over the years electroplated soft magnetic films (Ni-Fe-Co alloys [2-6] with high flux density and low coercivities have been extensively studied (shown in figure-1). These metallic alloys have high saturation flux density, low coercivity and high conductivity. The magnetic core is restricted by the skin depth (δ) equation ($\delta = \sqrt{\rho/\pi f \mu}$). Where, $\rho$, $f$, $\mu$ represents conductivity (Ω-m), operation frequency (Hz) and permeability (H/m) of the magnetic film. For thickness > δ, the flux is contained at the surface of the material and exponentially decreases towards the centre due opposing field generated by the induced current. Recent developments in soft sputtered films such as amorphous CoZrTa and CoZrO films have high resistivity ($\rho$ > 110 µΩ-cm) and saturation flux density ($B_{Sat}$ > 160 A/m) [7]. However, these materials do not retain soft magnetic properties on thick sputter deposition and patterning could be challenging. Hence, electrochemical process remains the most widely accepted process to deposit magnetic films. Attempts have been made to achieve laminated core structures with electrochemical process [8-9]. An analytical study with $Ni_{81}Fe_{19}$ (ρ: 24 µOhm-cm; laminated racetrack micro-inductors has been investigated. Micro-inductor footprint area (1 $mm^2$) and dimensions (core length: 0.75 mm; inductor length: 1.44 mm and inductor width: 0.7 mm and core thickness and spacer: 0.8 µm) have been kept fixed. Although the eddy current losses reduces, the core hysteresis loss increases with laminations which along with winding loss

then limits the efficiency for higher laminations (fig 2(a)). For high resistive soft-magnetic materials such as CZTB, lower number of laminations are needed compared to $Ni_{81}Fe_{19}$ to achieve same efficiency. Interestingly the micro-inductor operation frequency could also be increased on introducing core lamination (fig 2(b)). It is to be noted that the core relative permeability is considered frequency independent.

Authors have previously reported a surface activation method to metalize SU-8 50 dielectric [10]. In this work the authors exploited the process to fabricate magnetic multilayers by activating thinner SU-8 variant (SU-8 2). The experimental section will describe the SU-8 2 patterning, activation and metallization processes. The results and discussion will outline the characterization of laminated films for high-frequency applications and investigate the possible method of co-packaging the fabricated core in integrated microinductors and FEM analysis of the micro-inductor.

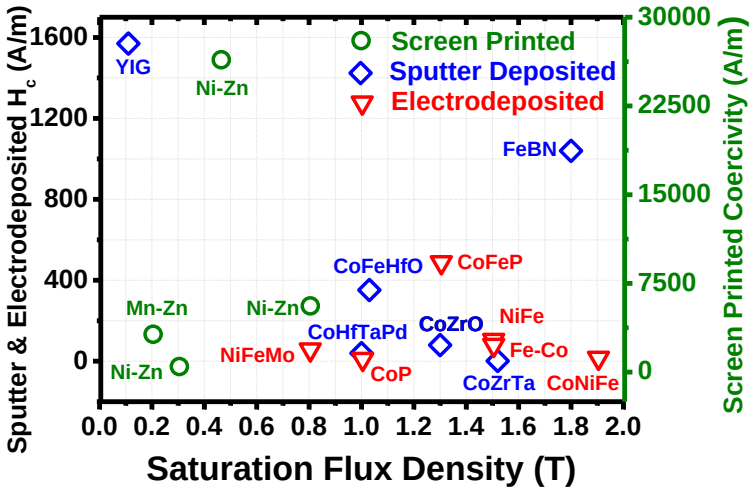


**Figure 1.** Coercivity vs saturation flux density of reported soft magnetic films.

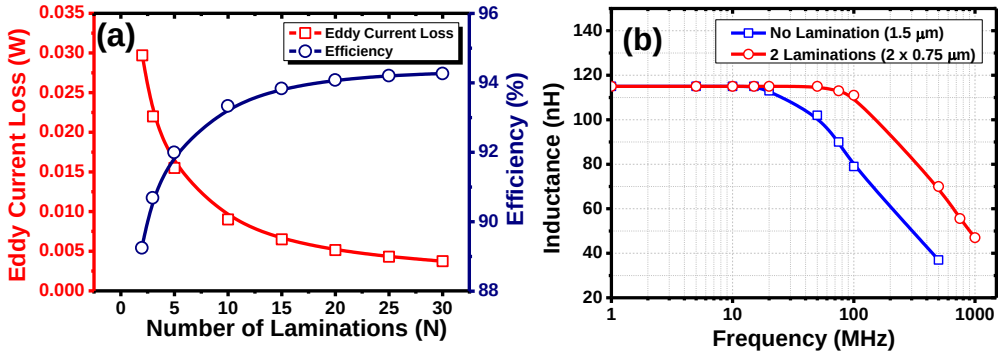


**Figure 2.** (a) Improvement in device efficiency and reduction in eddy current loss with number of lamination. (b) Inductance vs frequency curve with and without laminated micro-inductors.

## 2. Experimental Details

### *2.1. SU-8 2 Spin Coating*

It is important to have thin and pin-hole free spacers in-between ferromagnetic (FM) layers to achieve laminated cores. In this case SU-8 2, a thinner variant of SU-8 epoxy based photoresist is used as spacer layer. Fig. 3 depicts the spin speed vs thickness curves for different SU-8 variants as reported in the datasheet [11]. To achieve thickness ~ 1 µm, the main spin speed of 3000 rpm / 40 s is selected. Table-

1 details the process steps. The photoresist exposure was performed under Canon PLA-501 FA optical mask aligner in soft contact mode and resist thickness of 1 µm -1.5 µm was achieved (as measured in Tencor Alpha Step-200 surface profiler). This is followed by a short post exposure bake essential for cross-linking of SU-8 molecule in ramp mode to 65 ºC / 60 s and 95 ºC/ 60 s. In case of patterned samples, the resist is developed in EC solvent for 60 s.

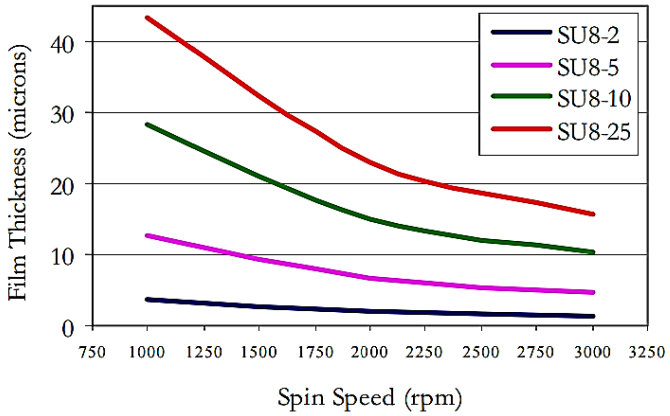


**Figure 3.** Spin speeds vs thickness curves for different variants of SU-8 (Obtained from datasheet [11]).

**Table 1.** SU-8 2 process steps

| **Process Steps** | **Quantity (mol-dm$^{-3}$)** |
|---|---|
| Spin profile | 100 rpm/ 10 s +500 rpm /10 s +3000 rpm/40 secs |
| Soft Bake | Ramp from 30 ºC to 95 ºC/ 3 mins |
| Exposure Dose | 100 mJ/cm$^2$ |
| Post-exposure bake | 65 ºC / 60 s + 95 ºC / 60 s |
| Development | 60 s in EC-solvent |

### *2.2. SU-8 2 Surface Activation and Electroless Deposition*

The surface of the SU-8 is plasma treated in oxygen plasma asher (March Plamod GCM-200) at 350 mW for 60 s to remove organic contaminants. This is followed by 1800 s of immersion in (3-Aminopropyl)-triethoxysilane (APTES) solution. A monolayer is formed on the SU-8, selectively binding the APTES to the activated epoxy group of SU-8 surface in a covalent bond. It is then immersed in a solution of palladium ions to form palladium nuclei on the SAM layer which can be reduced and is essential for activation of successive electroless chemical deposition [10, 12-13]. This is followed by electroless deposition of $Ni_{81}Fe_{19}$ in in-house developed bath in absence of external magnetic film. Table-II lists the bath constituents and deposition condition for electroless deposition of $Ni_{81}Fe_{19}$. This process is repeated sequentially (fig.4) to achieve laminated films to achieve 2 and 3 layers of $Ni_{81}Fe_{19}$ of thicknesses (~ 1.7 µm to ~ 3 µm) and 1 µm thick SU-8 2 spacers. It is however observed that $Ni_{81}Fe_{19}$ films > 2 µm show high stress.

**Table 2.** Borane based $Ni_{81}Fe_{19}$ bath constituents and deposition conditions

| Bath Contents | Quantity (mol-dm$^{-3}$) |
|---|---|
| Di-ammonium citrate | 0.027 |
| Lactic acid | 0.22 |
| $NiSO_4.6H_2O$ | 0.060 |
| $FeSO_4.7H_2O$ | 0.058 |
| DMAB | 0.034 |

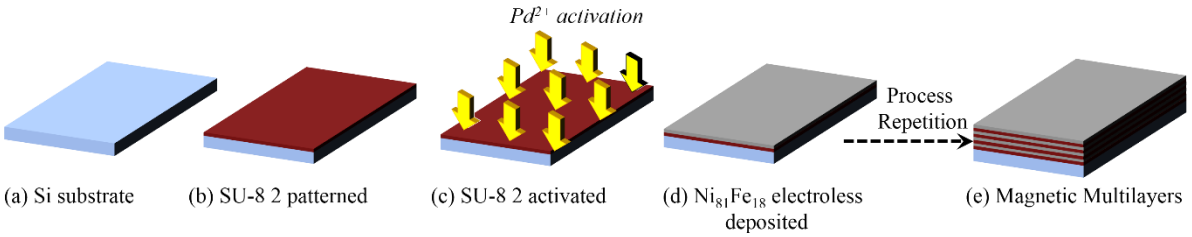


**Figure 4.** Spin speeds vs thickness curves for different variants of SU-8 (Obtained from datasheet

## 3. Results and Discussions

### *3.1. Characterizations*

The magnetic characterization of electroless $Ni_{81}Fe_{19}$ were measured on surface activated silicon films. Fig. 5(a) shows the hysteresis curve for ~ 250 nm thick $Ni_{81}Fe_{19}$ measured in BH loop tracer at 10 Hz (SHB Instruments, USA, Model: MESA 200 HF). As observed from the figure, the coercivity is higher (365 A/m) compared to electroplated $Ni_{81}Fe_{19}$ (< 100 A/m), which is one of the drawbacks with the process. However, a high anisotropy field > 1397 A/m measured on surface activated deposition. The relative permeability spectra measured with wide-band complex permeameter (Ryowa electronics, Japan, Model: PMM 9G) suggested a uniform response up to 600 MHz at null field (fig. 5(b)) for the 250 nm thick deposit. The increase in cut-off frequency ($f_c$) could be attributed to the lower thickness ($t$) and relative permeability ($\mu_r$) of the sample ($f_c \alpha \frac{1}{\mu_r t^2}$). Fig. 6 depicts the SEM micrograph of magnetic multilayers with sequential lithography-activation and deposition method. The shape of the sample (1mm x 3 mm) assists in uniform permeability, with high-frequency permeability characterization suggested uniform response up to 600 MHz, as observed in fig. 7.

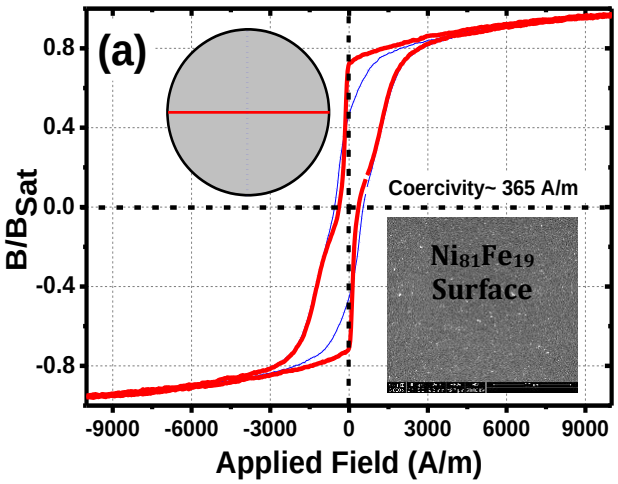

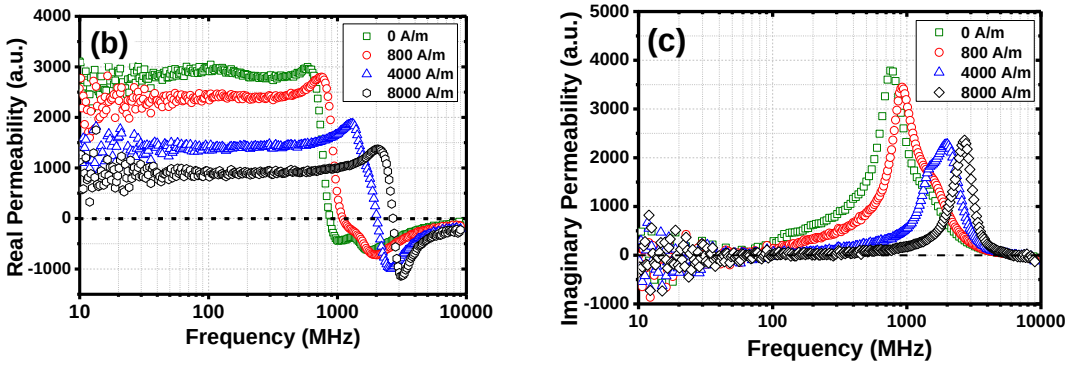


**Figure 5.** (a) Hysteresis loop of ~ 250 nm thick Permalloy films electrolessly deposited on surface activated silicon and its relative permeability vs frequency curves (3 mm x 3 mm).

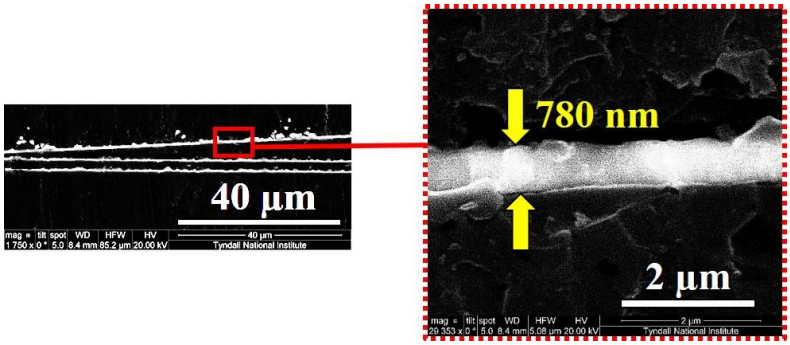


**Figure 6.** Cross-section SEM images of $Ni_{81}Fe_{19}$ mutli-layers with SU-8 2 spacers.

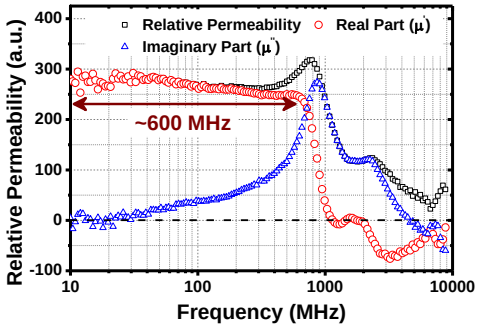


**Figure 7.** Initial permeability of 3 layers of $Ni_{81}Fe_{19}$ (~3 µm) and ~ 1 µm SU-8 spacer films (1 mm x 3 mm).

### *3.2. FEM Study of Solenoid Inductors with Co-Packaged Core*

In this section a possible solenoid inductor with packaged core structure is demonstrated. The above mentioned multilayer core structure can be co-packaged into an integrated device structure with fabricated bottom and top windings. The silicon substrate of the core multilayer structure is thinned and packaged with adhesive mould, followed by resist patterned. This is followed by wire-bonding top windings (fig.8). Fig. 9 depicts the inductance vs number of lamination curve for the device simulated with Maxwell Ansoft finite element method (FEM) from air-core (no lamination) to 10 laminations. As expected, there is increase in inductance with number of laminations. As the net core thickness increases,

this increase in inductance ceases. The future work involves optimizing the design and fabricating micro-inductors with co-packaged core.

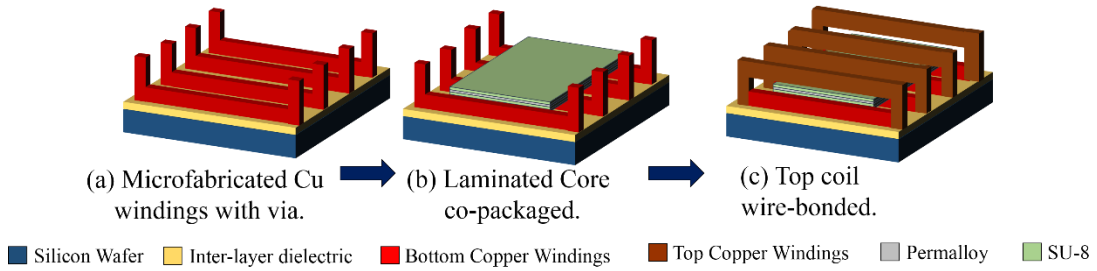


**Figure 8.** A schematic of fabricating solenoid inductors with co-packaged core.

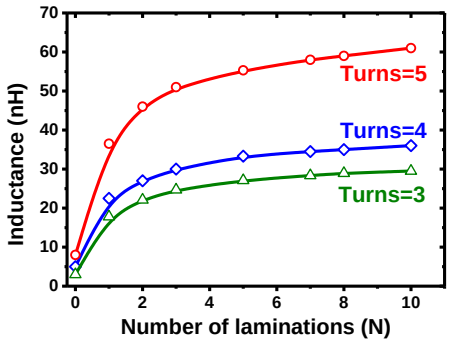


**Figure 9.** FEM simulated inductance vs lamination curve for 2 mm$^2$ laminated ($Ni_{81}Fe_{19}$: thickness: 0.8 µm separated by 1 µm SU-8 2) solenoid micro-inductor (3, 4 and 5 turns) with 5 mm core length.

## 4. Conclusions

We report a surface activation method to metallize SU-8 2 with soft magnetic material ($Ni_{81}Fe_{19}$). The magnetic measurements were conducted, which suggests a coercivity < 365 A/m. The high-frequency permeability tests showed uniform permeability response up to 600 MHz for 250 nm thick $Ni_{81}Fe_{19}$ on silicon. A sequential deposition of $Ni_{81}Fe_{19}$ on SU-8 2 to achieve magnetic multilayer is reported which showed improvement in frequency response with number of laminations. Finally, we propose a solenoid micro-inductor structure to with the co-packaged magnetic structure. FEM analysis suggested increase in inductance with laminations, which ceases with increase in net magnetic core thickness. The future work will involve details design study and optimization of the laminated device structure in terms of core shape and fabrication of solenoid micro-inductor.

### References

[1] Meere R, O'Donnell T, Wang N, Achotte N, Kulkarni S and O'Mathuna SC 2009 *IEEE Trans. Magn*. **45** 4234.
[2] Roy S et. al., 2005 *J. Magn. Magn. Mater*. **290-291** 1524.
[3] Rhen MF, McCloskey P, O'Donnell T and Roy S 2008 *J. Magn. Magn. Mater*. **320** e819.
[4] McCloskey P et. al., *J. Magn. Magn. Mater*. **320** 2509.
[5] Park JY and Allen MG 1999 *5th IEEE Symp. Mag. Mater*. 389.
[6] Myung NV et. al. 2003 *J. Magn. Magn. Mater*. **265** 189.
[7] Gardner DS et. al. 2009 *IEEE T. Magn*.**45** 4790.
[8] Brunet M, O'Donnell T, Connell AM, McCloskey P and O'Mathuna SC 2006 *IEEE Trans. Micromech. Syst*. **15** 94.

[9] McCloskey P, Jamieson B, O'Donnell T, Gardner D, Morris MA and Roy S 2008 *J. Magn. Magn. Mater*. **320** 2509.
[10] Anthony R, Rohan JF and O'Mathuna C 2016 *Microelec. Engg.* **155** 33.
[11] SU-8 Datasheet (http://www.microchem.com/pdf/SU8_2-25.pdf ).
[12] Anthony R, Shanahan BJ, Waldron F, O'Mathuna C and Rohan JF 2015 *Appl. Surf. Sci.* **357** 385.
[13] Anthony R, O'Mathuna C and Rohan JF 2015 *Proc. Phys.* **75** 1207.

**Acknowledgments**
The authors acknowledge European Union for funding the research work through project through FP-7 (Project: PowerSwipe) under grant agreement no.: 318529 for the support and Central Fabrication Facilities (CFF) for the support.